Helical magnetic fields in the M87 jet at arc-second scales

J. C. Algaba, K. Asada and M. Nakamura

Academia Sinica, Institute of Astronomy and Astrophycis, P.O Box 23141, Taipei 10617, Taiwan

Received _____; accepted _____

ABSTRACT

We investigate the magnetic field configuration of the M87 jet at arc-second scales by using archival polarimetric VLA data at 8, 15, 22 and 43 GHz. By stacking images over three years in order to enhance the sensitivity, we reveal, for the first time, systematic transverse gradients of the Faraday rotation measure in several knots along the jet. Combining this result with polarization properties and the dynamics of the jet, we suggest the magnetic structure in several knots at kiloparsec scales consists of a systematically wrapped, tightly wound helical configuration. Our analysis brings us a new paradigm where the M87 jet is a fundamentally current carrying system produced in the vicinity of the supermassive black hole, transferring a huge amount of the electromagnetic energy over the host galaxy scale.

Subject headings: galaxies: active — galaxies: individual (M87) — galaxies: jets — polarization

1. Introduction

M87 hosts a supermassive black hole (SMBH) with $M_\bullet = (3.2 - 6.6) \times 10^9 M_\odot$ (Macchetto et al. 1977; Gebhardt et al. 2011; Walsh et al. 2013). It is one of the closest active galactic nuclei (AGNs) at a distance $D = 16.7$ Mpc (Tonry 1991) with an extended jet. The origin of the jet emission is synchrotron from radio through optical to X-ray (see e.g., Biretta et al. 1991; Perlman et al. 2001; Harris et al. 2003). With an angular scale of 78 pc arcsec^{-1} and viewing angle of $\theta = 10^\circ - 19^\circ$ (see e.g., Biretta et al. 1999; Wang & Zhou 2009)[1], the M87 jet has been intensively studied as one of the best references in AGN jets.

High dynamic range and high resolution images were first obtained with VLA more than thirty years ago (Owen et al. 1980). Since then, observations have revealed more detailed morphology of the jet in optical and radio bands (see e.g., Owen et al. 1989; Perlman et al. 1999). It is becoming clear that hydrodynamics alone may not be able to produce the rich structure in total and polarized intensities; knots cannot be associated with Kelvin-Helmholtz instabilities (Hardee & Eilek 2011). In turn, magnetic fields appear to organize the jet structure in M87 (see e.g. Owen et al. 1989; Perlman et al. 1999, 2001). Nonetheless, the magnetic structure and its dynamical role are still unclear.

Strong polarization reaching almost the maximum in synchrotron radiation ($> 60\%$) has been found on kiloparsec scales (Owen et al. 1990; Perlman et al. 1999), suggesting magnetic fields are ordered. The core, however, is highly unpolarized ($< 0.4\%$) in radio bands (Homan & Lister 2006). Polarization seems to behave differently in optical and radio bands: magnetic vector orientations are perpendicular to the direction of the jet in knots

[1]Through this letter we use $\theta \sim 15^\circ$ (Wang & Zhou 2009).

HST-1, D, E and F[2] in optical but remains parallel in radio wavelengths (Perlman et al. 1999).

A way to study the structure of the intrinsic magnetic field is the analysis of the Faraday rotation measure distribution across the source. The polarization angle χ rotates following the relation $\chi = \chi_0 + \mathrm{RM}\lambda^2$, where χ_0 is the intrinsic polarization angle, λ the wavelength and RM the rotation measure, given by

$$\mathrm{RM} \propto \int n_e B_{los} \cdot dl \tag{1}$$

with n_e the thermal electron density and $B_{los} \cdot dl$ the line of sight component of the magnetic field.

If the jet contains a helical magnetic field, its toroidal component will produce a gradient, and possibly a sign reversal, on the RM across the jet, (Blandford 1993). Such gradients have been observed in a variety of sources (see e.g., Asada et al. 2002; Gabuzda 2004; Zavala & Taylor 2005; Gómez et al. 2008; Mahmud et al. 2009; Croke et al. 2010; Hovatta et al. 2012; Algaba 2013). RMs are observed systematically on parsec scale of AGN(Hovatta et al. 2012) although, due to polarization errors and beam effects, the limits of their reliability and interpretation are still under debate. However, no significant transverse RM gradient has been observed in the M87 jet on any scale so far.

A rotation of the polarization angle of $\sim 75^\circ$ between optical and 6 cm over 20 arcseconds in M87 was found by Schmidt et al. (1978) and confirmed by Dennison (1980). RM observations of M87 were performed with the VLA using 5 GHz band by Owen et al. (1990), who found high values (RM$\sim 1000 - 2000$ rad m^{-2}) in the lobes and lower (RM~ 200 rad m^{-2}) in the jet. Their interpretation was the existence of a Faraday screen

[2]Here we follow the traditional notation (see e.g. Perlman et al. 2001) to name the different features in the kiloparsec scale of the M87 jet.

consisting on a thick layer enveloping the radio lobes with the jet lying mostly in front of it. Zavala & Taylor (2003) found RM at milli-arc second scales with indications of a change of sign, interpreted as due to hot gas and narrow line region clouds.

We report here our study via image stacking of a series of multi–frequency polarimetry on VLA archives. We describe the archival data reduction in section 2. We present observational results in section 3, their implementation as helical magnetic fields in section 4. Discussion and conclusions are given in sections 5 and 6.

2. Archival data reduction

We analyzed six different epochs of VLA multi–frequency polarization observations of M87 obtained from the archive[3]. We summarize the observations in Table 1, where we include the frequencies used, the VLA configuration and the observations date. Data were reduced in AIPS[4] using standard methods. We corrected for the intrinsic antenna polarization (D–terms) with the sources 0521+166 and 1224+035 as calibrators and for the polarization angle using 3C 286 as calibrator. We then imaged the source.

After the initial construction of total intensity maps we used the final calibrated visibilities to obtain maps of the Stokes Q and U distributions. Those were used to construct the polarized flux ($p = \sqrt{Q^2 + U^2}$) and polarization angle [$\chi = (1/2)\arctan(U/Q)$] maps. In all cases we compared the polarization vectors with 3C 286. We then stacked the images obtained at the different epochs weighting them by their rms noise. Final images at 8, 15, 22 and 43 GHz convolved with a beam of FWHM of $0.23''$ were used to construct the RM

[3]`https://archive.nrao.edu`

[4]Astronomical Image Processing System, developed and maintained by the National Radio Astronomy Observatory

map.

3. Rotation Measure and Polarization

We show the RM map in Figure 1, where upper and lower maps stand for the RM values and errors respectively, using the color scale indicated on top of the figure. Faraday–corrected magnetic field vectors are also shown. Regions where polarization below $p = 3\sigma$ for 8 GHz or RM is not corrected are not shown. We detect RMs of several thousands rad m^{-2} in HST-1 and of several hundreds rad m^{-2} in knots A, B and C. Except for HST-1, the regions where the RM is found extend more than two beams both along and across the jet. A clear RM gradient across the jet is seen in HST-1 and knots A and C, but a more patchy behavior is seen in knot B.

In order to investigate these, we have taken slices across the jet (see Figure 2). In all cases where a gradient is clearly seen, the RM runs smoothly from positive values in the north to negative values in the south side of the jet. Simple analysis indicates that these gradients in HST-1 and knots A and C fulfill the robustness criteria given in the literature (Hovatta et al. 2012; Mahmud et al. 2013; Algaba 2013). We also confirm that no gradient is detected in knot B. Relative errors for the gradients, taken as err(RM)/[RM$_{max}$−RM$_{min}$], are roughly 8%, 21% and 25% for HST-1 and knots A and C respectively. This indicates that, even for HST-1, with the RM barely extending one beam size, relative error is small enough to indicate the robustness of this gradient. Such a systematic transverse gradient has never been seen along various regions on kiloparsec scales of the M87 jet. We succeeded to derive it thanks to our image stacking, wide range in the λ^2 space and high resolution.

Faraday–corrected polarization (see Figure 1) tends to be aligned with the direction of the jet. Where the jet bends after knot B, polarization follows this bend. Two exceptions

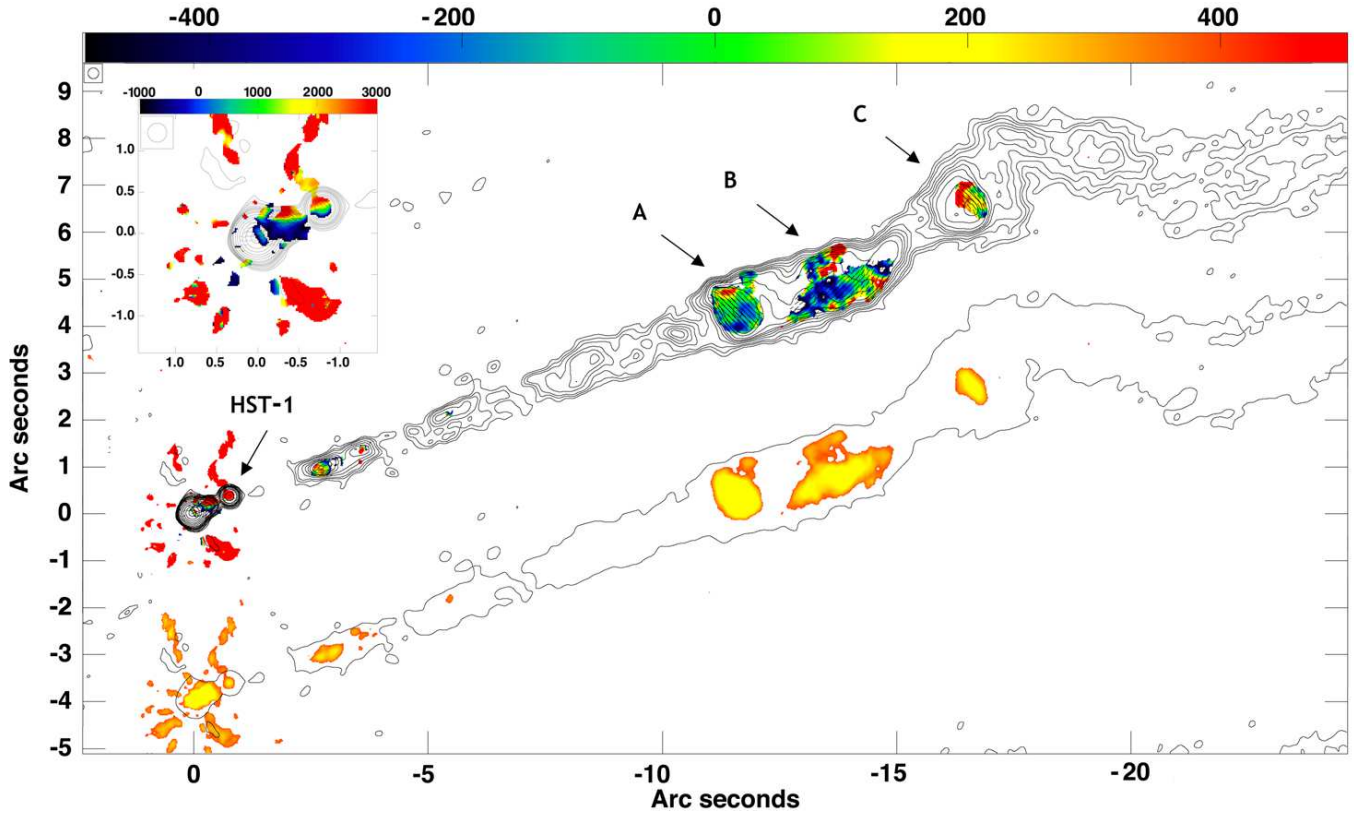

Fig. 1.— Rotation measure and polarization map of the M87 jet. Contours indicate total intensity for 8 GHz, starting at 2×RMS with RMS=1.13×10^{-3} and increasing in steps of (2, 3, 4, 6, 8, 10, 12, 16, 24, 32, 64, 128, 256, 512). Sticks indicate the Faraday corrected magnetic field direction. No polarization sticks are shown for SNR<3. Color indicates RM, upper and lower maps showing RM and RM errors respectively, from -500 to 500 rad m^{-2}, as indicated by the top bar. In the top left corner, a plot of the RM of knot HST-1 is shown with a different scale (from -1000 to 3000 rad m^{-2}) for clarity.

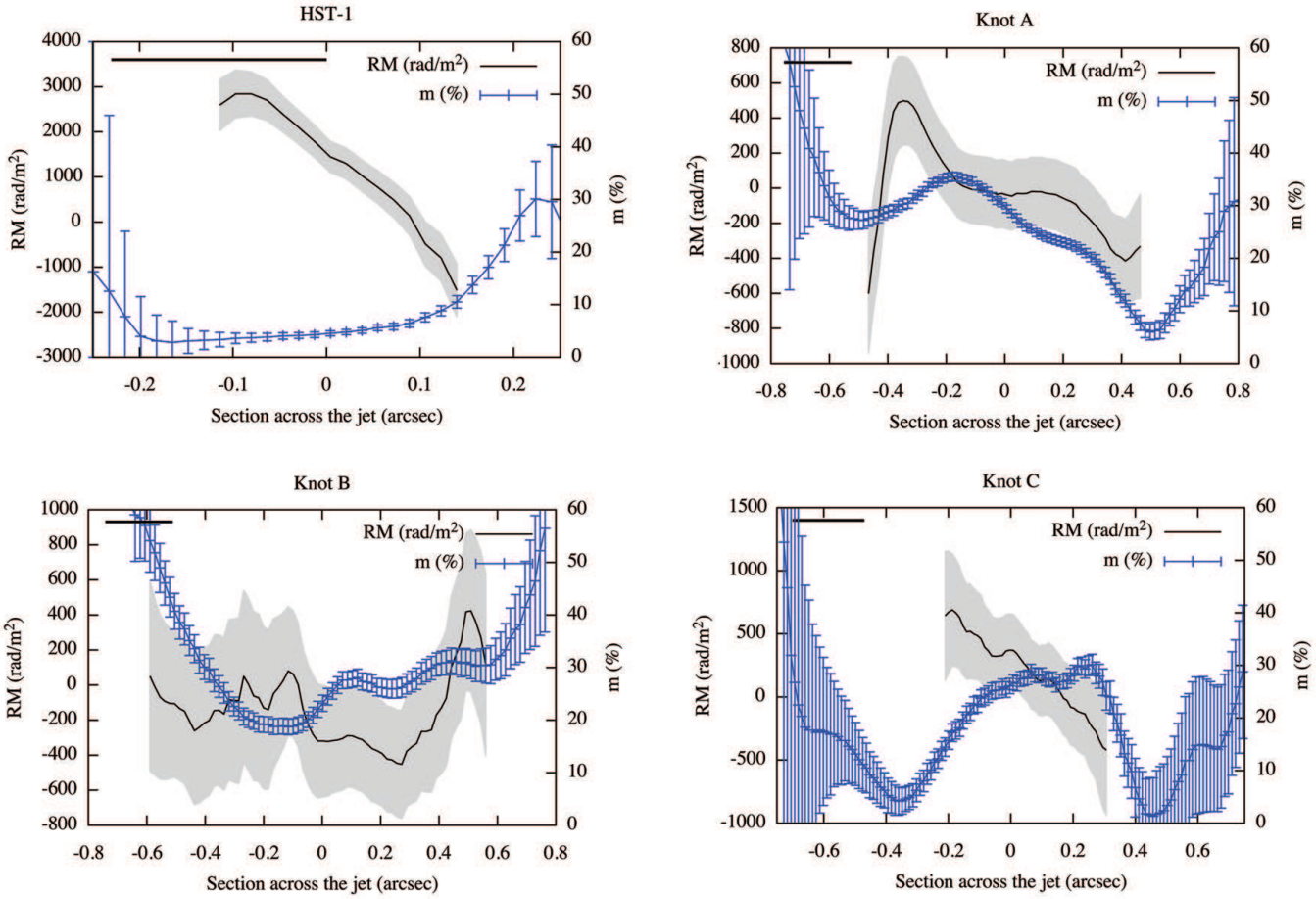

Fig. 2.— Slices of degree of polarization and RM across the jet in HST-1 and knots A, B and C. Black line with shaded area indicates the RM value and its error, whereas blue line indicates the degree of polarization. The black thick line in the top left corner indicates the beam size in each region.

are knots A and C, where polarization appears almost perpendicular to the direction of the jet. This is in agreement with previous results by Owen et al. (1989) although they corrected for Faraday rotation using only 6 cm data. When examining the polarization of knot A, Owen et al. (1989) found a bow-shock shape (i.e, although a spine-sheath morphology is not clear, magnetic polarization angles tend to rotate towards the direction of the jet as it approaches the edges). As we correct for RM on a wider range of radio frequencies, this effect is much less evident in our map and only a slight bend can be found.

Fractional polarization shows a tendency of increasing towards the jet edges up to $m \sim 50\%$ (Figure 2) and is also higher at the centre of the jet in knots A and C (This has also been observed in other sources such as 1055+018 (Attridge et al. 1999), NGC 315 (Laing et al. 2006b) or 1633+382 (Algaba 2013), for example). Distribution of fractional polarization seems to be asymmetric across the jet axis in all regions, although HST-1 is not resolved and its transverse profile might be partially smoothed by beam convolution. Such asymmetric increase of m towards the edges of the jet is expected if we consider a helical magnetic field viewed at a certain angle (Gómez et al. 2008; Agudo et al. 2012). The higher fractional polarization in the centre of the jet has also been modeled in this context (Laing et al. 2006a). This scenario can also arise if we have a shock where a random magnetic field intrinsically weakly polarized is compressed in a plane (e.g., Laing 1980). However, as Nakamura et al. (2010) pointed out, the classical picture of a weak, random jet magnetic field may be in conflict with observations showing high degree of polarization (typically $> 10\%$) even at interknot regions of the M87 jet (Sparks et al. 1996).

4. Helical Magnetic Fields

4.1. Rotation Measure Gradients as Tracers of Helical Magnetic Fields

This is the first time transverse gradients of RM are systematically discovered in various regions of kiloparsec scales along the M87 jet. Such smooth gradients including a change of sign are difficult to be explained by an alternative phenomena such as electrons distribution, but arises naturally as the change of the line of sight components of the magnetic field across the jet.

There is a possibility that the RM gradient might be associated with the foreground medium. For example, there may be some amount of Faraday screen associated with the lobe after knot C. We suggest this is unlikely for HST-1 and knots A, B and C. If the RM arises from an external Faraday screen, likeliness of it being consistent with this picture by chance can be estimated as follows: Let us consider for simplicity only the sign of the RM on both sides across the jet as a fiducial indicator of a gradient. In this case, probability of having a change on the RM sign on HST-1 and the same one on knots A and C, but not on knot B is $p = 1/2 \times 1/4^2 \times 1/2 < 2\%$. We note that here we did not account for gradient smoothness, which is clear in our observations.

Therefore, observed RM gradients suggests the presence of a helical magnetic field in knots A, C and HST-1, while the magnetic field in component B, if also helical, should be much more loosely wound (note we would reject a possibility of random magnetic field due to its high degree of polarization). This indicates that the M87 jet may be a strongly magnetized even at kiloparsec scales and thus the magnetohydrodynamic (MHD) properties should be taken into account for understanding of the M87 jet.

4.2. A Constraint of Helical Magnetic Field Pitch Angles

If we assume a helical magnetic field in the M87 jet, we can obtain a constraint for the magnetic pitch angle $\psi = \arctan(B_\phi/B_z)$, where B_ϕ is the azimuthal and B_z the axial component. (Asada et al. 2002). For a given viewing and pitch angles, we can decompose the magnetic field component along the line of sight as $B_{los} = B_\phi \cos\theta + B_z \sin\theta$. In order to have both signs of RM for HST-1 and knots A and C, this suggests $\psi \gtrsim 75°$. On the other hand, the lack of a clear gradient in knot B may indicate that here the toroidal component does not dominate and we suggest $\psi \lesssim 75°$ for knot B.

The presence of polarization parallel or perpendicular to the jet can be explained with a helical magnetic field with variations of the viewing angle θ and/or magnetic pitch angle ψ (Asada et al. 2002). In this model, we observe polarized emission from both front and rear of the emitting regions, but polarization angles have a 180°offset. When both contributions are geometrically added, the result depends on the pitch angle of the jet. For a small ψ, the longitudinal component of the magnetic field dominates and resulting magnetic angle will be parallel to the jet, whereas for a large ψ, the toroidal component dominates and the magnetic polarization angle will be perpendicular to the jet. Thus, assuming a helical magnetic field, the threshold between the two possibilities will be given by $B_\phi/B_z = \sin\theta$ (Asada et al. 2008).

From here we can obtain a second constraint for ψ. Taking the viewing angle $\theta = 15°$, the magnetic polarization angles imply a lower limit for $\psi \gtrsim 15°$ for HST-1 and knots A and C and an upper limit $\psi \lesssim 15°$ for knot B. This result agrees with the one previously discussed based on the RM in HST-1 and knots A, B and C, which suggests that observed Faraday rotation is associated with jet and not with a foreground medium.

Combining the constraints for the magnetic pitch angle both from RM and magnetic polarization angle together, we obtain $\psi \gtrsim 75°$ for HST-1 and knots A and C and $\psi \lesssim 15°$

for knot B. This seems to indicate that knots A and C are shocks where the gas and magnetic fields are compressed, whereas knot B is the post-shocked region.

5. Discussion

5.1. A/B/C Complex as Quad MHD Shock System

According to a MHD model for the M87 jet (Nakamura et al. 2010), a series of MHD quad shocks may be originated at the HST-1 complex by an over-collimation. Initiated shocks propagate downstream of HST-1, and a pair of forward (superluminal) and reverse (subluminal) features are observed (Biretta et al. 1999; Cheung et al. 2007; Giroletti et al. 2012). Nakamura et al. (2010) propose that quasi-periodic (D, E, F/I, and A/B/C) knot complexes are a consequence of reverse/forward fast MHD shocks. Morphology of the M87 jet in arcsecond scales seems to support this, as several complexes can be identified with quad shock systems (see Figure 1). Under this context, knots A and C are twin features, corresponding to the forward and reverse MHD fast mode shocks, whereas knot B would be the post-shocked region. An asymmetric distribution of the fractional polarization normal to the jet axis may also indicate a forward/reverse shock feature. By considering a conical expansion of the kiloparsec scale M87 jet, $\psi \sim 88^\circ$ at the knot A is estimated (Nakamura et al. 2010), in agreement with the lower limit $\psi \gtrsim 75^\circ$ proposed here.

Very recently, Meyer et al. (2013) studied proper motions of the M87 jet at arcsecond scales by using more than a decade of HST archival imaging. Significant apparent motions $\gtrsim c$ are newly found at the A/B/C complex; knots A and C move to opposite direction transverse to the jet axis. This may indicate a counter-rotational motion around the jet axis as expected in a MHD quad shock system. Overall velocity profiles along the jet as well as transverse to the jet axis in Meyer et al. (2013) may be explained as embedded flow

trajectories within systematic helical magnetic fields. Component velocities upstream of knot A have still highly relativistic and thus one-sided transverse motions (Doppler boosted towards us) are observed. Once the jet becomes mildly relativistic, we are able to follow the full motion of helical patterns; there is a conspicuous 'tip-to-tail' alignment of almost all the velocity vectors within the knot A/B/C complex, strongly suggesting a flattened view of a helical motion which might result in such a 'zig-zag' pattern (Meyer et al. 2013). Furthermore, these paired MHD fast mode shocks at knots A and C may be responsible for driving the kinked structure at around the post shock region of knot B by the current-driven instability (Nakamura & Meier 2004). We thus suggest that the region A/B/C could be a good example for the interplay between the MHD shocks and current-driven instability where the magnetic field plays a role in the jet dynamics.

5.2. The M87 Jet as a Current Carrying System

Given a helical magnetic field along the jet, there will be an associated axial electric current I_z. Following Kronberg et al. (2011) with a fiducial value of the toroidal field strength B_ϕ and the jet radius r of knot A (e.g. Owen et al. 1989; Stawarz et al. 2005), we estimate

$$I_z \simeq 4.6 \times 10^{17}\,\mathrm{A}\,\left(\frac{B_\phi}{500\,\mu\mathrm{G}}\right)\left(\frac{r}{60\,\mathrm{pc}}\right). \tag{2}$$

On the other hand, assuming an equipartition field strength of $\sim 10^3$ G at the Schwarzschild radius $r_s = 2GM_\bullet c^{-2}$ for $M_\bullet = 3.5 \times 10^9 M_\odot$ (Walsh et al. 2013), the current, generated in the vicinity of the SMBH, can be estimated as

$$I_z \simeq 5.1 \times 10^{18}\,\mathrm{A}\,\left(\frac{B_\phi}{10^3\,\mathrm{G}}\right)\left(\frac{r_s}{3.3 \times 10^{-4}\,\mathrm{pc}}\right). \tag{3}$$

Therefore, it seems that the electric current is being carried from the SMBH to beyond the host galaxy in M87 over $10^7\,r_s$ scales without a considerable dissipation.

The electromagnetic power, advected with knot A, can be estimated as

$$L \simeq 3.2 \times 10^{43}\,\mathrm{erg\,s^{-1}} \left(\frac{r}{60\,\mathrm{pc}}\right)^2 \left(\frac{B_\phi}{500\,\mu\mathrm{G}}\right)^2 \left(\frac{V_z}{c}\right). \quad (4)$$

This is comparable to the total jet power in the literature (e.g. Reynolds et al. 1996; Owen et al. 2000; Stawarz et al. 2005). Thus, we speculate the electromagnetic energy is channeled throughout the whole extension of the jet in M87. Sizes of X-ray cavities in M87 about ~ 1 kpc (Rafferty et al. 2006) could be supported by the current-dominated bubble expansions, requiring $I_z \sim 10^{18}$ A (Diehl et al. 2008). Thus, a current-carrying, magnetized jet may be relevant for the overall energetics in the M87 jet and lobe system.

6. Conclusions

We have collected archival data to study multifrequency (8+15+22+43 GHz) VLA polarization images of the M87 jet. By image stacking, the use of a wide range in the λ^2 domain and a resolution of 0.23 arcseconds, we are able to detect, for the first time, rotation measure gradients across the the M87 jet on various knots at arcsecond scales. Faraday corrected magnetic angles clearly follow the jet direction, except for HST-1 and knots A and C, where they appear to be perpendicular to it.

In order to study polarimetric properties, slices of fractional polarization and RM across the jet were taken. These support that RM gradients are reliable in HST-1 and knots A and C, but no detection of a gradient is found in knot B. Indications of an increase of fractional polarization towards the edges are seen in HST-1 and knots A, B and C; with knots A and C showing additional higher fractional polarization in the centre of the jet.

The most natural way to explain the combined information from i) RM transverse gradients, ii) magnetic position angles, iii) the high fractional polarization, showing a clear transverse asymmetry and increasing towards the edges of the jet and iv) jet dynamical

transverse velocities (Meyer et al. 2013), is the presence of a helical magnetic field in the jet of M87. In this picture, the magnetic configuration of the M87 jet consists of a systematically wrapped, tightly wounded, helical structure extending at least from 0.1 to 1 kiloparsec from HST-1 to knot C, supporting a MHD model in the M87 jet (Nakamura et al. 2010).

The presence of a systematic helical magnetic field at least a kiloparsec along the M87 jet brings us a new paradigm to describe AGN jets as fundamentally electromagnetic, current carrying systems. It also indicates transferring a huge amount of energy, made by the black hole magnetosphere, in the form of Poynting flux, and depositing it into the surrounding galactic environment.

We are grateful to R. Laing and the ASIAA VLBI group for valuable discussion and the anonymous referee for useful comments. The National Radio Astronomy Observatory is operated by Associated Universities, Inc., under contract with the National Science Foundation.

Table 1: Observing Sessions.

Obs. Code	Freq. (GHz)	VLA Conf.	Date
(1)	(2)	(3)	(4)
AH822A	8, 15, 22	A	2 Jun 2003
AH822B	8, 15, 22	A	24 Aug 2003
AH822C	15, 22, 43	B	16 Nov 2003
AH862A	8, 15, 22	A	15 Nov 2004
AH862B	8, 15, 22	A	31 Dec 2004
AH862C	15, 22, 43	B	3 May 2005

REFERENCES

Agudo, I., Gómez, J. L., Casadio, C., Cawthorne, T. V., Sogorb, M. R., 2012, ApJ, 752, 92

Algaba, J. C., 2013, MNRAS, 429, 3551

Asada, K., Inoue, M., Uchida, Y., Kameno, S., Fujisawa, K., Iguchi, S., Mutoh, M., 2002 PASJ, 54, L39

Asada, K., Inoue, M., Nakamura, M., Kameno, S., Nagai, H. 2008, ApJ, 682, 798

Attridge J. M., Roberts D. H., Wardle J. F. C., 1999, ApJ, 518, 87

Blandford, R. D. in Astrophysical Jets, ed. D. Burgarella, M. Livio, & C. P. O'Dea Cambridge: Cambridge Univ. Press (1993)

Biretta, J. A., Stern, C. P., Harris, D. E., 1991 AJ, 101, 1632

Biretta, J. A., Sparks, W. B., Macchetto, F., 1999 ApJ, 520, 621

Cheung, C. C., Harris, D. E., Stawarz, Ł, 2007, ApJ, 663, 65

Croke, S. M., OSullivan, S. P., Gabuzda, D. C. 2010, MNRAS, 402, 259

Dennison, B., 1980, ApJ, 236, 761

Diehl, S., Li, H., Fryer, C. L., Rafferty, D., ApJ, 687, 173

Gabuzda D. C., Murray, E., Cronin, P., 2004, MNRAS, 351, 89

Gebhardt, K., Adams, J., Richstone, D., Lauer, T. R., Faber, S. M., Gültekin, K., Murphy, J., Tremaine, S. 2011, ApJ, 729, 119

Giroletti, M., Hada, K., Giovannini, G., Casadio, C., Beilicke, M., Cesarini, A., Cheung, C. C., Doi, A., Krawczynski, H., Kino, M., Lee, N. P., Nagai, H., 2012 A&A 538, 10

Gómez, J. L., Marscher, A. P., Jorstad, S. G., Agudo, I., Roca-Sogorb, M., 2008, ApJ, 681, L69

Hardee, P. E., Eilek, J. A., 2011, ApJ, 735, 61

Harris, D. E., Biretta, J. A., Junor, W., Perlman, E. S., Sparks, W. B., Wilson, A. S., ApJ, 586, 41

Homan, D. C. & Lister, M. L., 2006 AJ, 131, 1262

Hovatta, T., Lister, M. L., Aller, M. F., Aller, H. D., Homan, D. C., Kovalev, Y. Y., Pushkarev, A. B., Savolainen, T. , 2012, AJ, 144, 105

Kronberg, P. P., Lovelace, R. V. E., Lapenta, G., Colgate, S. A., 2011, ApJL 741, L15

Laing, R. A., 1980, MNRAS, 193, 439

Laing, R. A., Canvin, J. R., Bridle, A. H., in Proceedings of the International Conference: "The Origin and Evolution of Cosmic Magnetism" 2006a; eds R. Beck, G. Brunetti, L. Feretti, and B. Gaensler

Laing, R. A.; Canvin, J. R.; Cotton, W. D.; Bridle, A. H., 2006b MNRAS, 368, 48

Mahmud, M.; Gabuzda, D. C.; Bezrukovs, V., 2009, MNRAS, 400, 2

Mahmud, M.; Coughlan, C. P.; Murphy, E.; Gabuzda, D. C.; Hallahan, D. R., 2013, MNRAS43, 695

Macchetto, F., Marconi, A., Axon, D., Capetti, A., Sparks, W., Crane, P. 1997, ApJ, 489, 579

Meyer, E., Sparks, W. B.; Biretta, J. A., Anderson, J., Sohn, S. T., Van Der Marel, R. P.; Norman, C. A., Nakamura, M. 2013, ApJL, 774, L21

Nakamura, M., Meier, D. L., 2004, ApJ, 617, 123

Nakamura, M.,Garofalo, D., Meier, D. L., 2010, ApJ721, 1783

Owen, F. N., Hardee, P. E., Bignell, R. C., 1980, ApJ, 239, L11

Owen, F. N., Hardee, P. E., Cornwell, T. J., 1989, ApJ, 340, 698

Owen, F. N., Eilek, J. A., Keel, W. C., 1990, ApJ, 362, 449

Owen, F. N.; Eilek, J. A.; Kassim, N. E., 2000 ApJ543, 611

Perlman, E. S., Biretta, J. A., Zhou, F., Sparks, W. B., Macchetto, F.D., 1999, ApJ, 117, 2185

Perlman, E. S., Biretta, J. A., Sparks, W. B., Macchetto, F.D., Leahy, J.P., 2001, ApJ, 551, 206

Rafferty, D. A.; McNamara, B. R.; Nulsen, P. E. J.; Wise, M. W., ApJ, 652, 216

Reynolds, C. S., Fabian, A. C., Celotti, A., Rees, M. J., MNRAS283, 873

Schmidt, G. D., Peterson, B. M., Beaver, E. A., 1978, ApJ, 220, L31

Sparks, W. B., Biretta, J. B., Macchetto, F, 1996, ApJ, 473, 254

Stawarz, Ł., Siemiginowska, A., Ostrowski, M., Sikora, M. 2005, ApJ, 626, 120

Tonry, J. L., 1991 ApJL, 373, L1

Walsh, J. L., Barth, A. J., Ho, L. C., Sarzi, M, 2013, ApJ770, 86

Wang, C. C., Zhou, H. Y., 2009, MNRAS, 395, 301

Young, A. J., Wilson, A. S., Mundell, C. G. 2002, ApJ, 579, 560

Zavala, R. T. & Taylor, G. B., 2002, ApJ, 589, 126

Zavala, R. T. & Taylor, G. B., 2005, ApJ, 626, 73

This manuscript was prepared with the AAS LaTeX macros v5.2.